Toy models of crossed Andreev reflection

2003 J. Phys.: Condens. Matter 15 5591

(http://iopscience.iop.org/0953-8984/15/32/318)

INSTITUTE OF PHYSICS PUBLISHING JOURNAL OF PHYSICS: CONDENSED MATTER

J. Phys.: Condens. Matter **15** (2003) 5591–5598 PII: S0953-8984(03)63081-X

Toy models of crossed Andreev reflection

R Mélin[1], **H Jirari**[1] **and S Peysson**[2]

[1] Centre de Recherches sur les Très Basses Températures (CRTBT)[3], CNRS BP 166X, 38042 Grenoble Cedex, France
[2] Instituut voor Theoretische Fysica, Universiteit van Amsterdam, Valckenierstraat 65, 1018XE Amsterdam, The Netherlands

E-mail: melin@polycnrs-gre.fr

Received 1 May 2003
Published 1 August 2003
Online at stacks.iop.org/JPhysCM/15/5591

Abstract

We propose toy models of crossed Andreev reflection in multiterminal hybrid structures containing out-of-equilibrium conductors. We apply the description to two possible experiments: (i) to a device containing a large quantum dot inserted in a crossed Andreev reflection circuit, and (ii) to a device containing an Aharonov–Bohm loop inserted in a crossed Andreev reflection circuit.

1. Introduction

The transport of correlated pairs of electrons in solid state devices has attracted intense interest recently. Due to progress in the fabrication of nanoscopic devices it will soon be possible to realize transport experiments in which two normal metal or spin polarized electrodes are connected to a superconductor within a distance smaller than the BCS coherence length. Transport theory of multiterminal hybrid structures has been investigated recently with various methods (a scattering approach in [1], lowest-order perturbation in [2], and the Keldysh formalism in [3]). Multiterminal hybrid structures can be used to manipulate entangled pairs of electrons in solid state devices [1–8] and will allow new tests of quantum mechanics with electrons such as EPR [4, 5, 8] or quantum teleportation experiments [7].

It has been suggested recently [9] that proximity effect experiments at a ferromagnet/superconductor interface could be explained by spatially separated Cooper pairs in which the spin-up (spin-down) electron propagates in a spin-up (spin-down) domain. This gives a strong motivation for investigating new situations involving spatially separated pairs of electrons, which we do in this paper. One of the possible experiments that we propose involves a large quantum dot inserted into a crossed Andreev reflection circuit. This device can be used to probe spin accumulation related to crossed Andreev reflection and elastic cotunnelling. Another device that we propose involves an Aharonov–Bohm loop inserted into a crossed Andreev reflection circuit. This device can be used to probe Aharonov–Bohm oscillations

[3] UPR 5001 du CNRS, Laboratoire Conventionné avec l'Université Joseph Fourier.

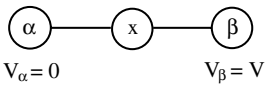

Figure 1. The toy model used to discuss the interplay between elastic cotunnelling and sequential tunnelling. The local chemical potential at node x is determined in such a way that current is conserved.

associated with spatially separated pairs of electrons. By crossed Andreev reflection we mean the possibility that a spin-up electron from a spin-up ferromagnetic electrode is Andreev reflected as a spin-down hole in another spin-down ferromagnetic electrode on the condition that the distance between the ferromagnetic electrodes is sufficiently small. The other possible process is elastic cotunnelling, in which a spin-up electron from a spin-up ferromagnetic electrode is transferred as a spin-up electron into another ferromagnetic spin-up electrode. With a partially polarized ferromagnet, crossed Andreev reflection can take place in the parallel alignment and elastic cotunnelling can take place in the antiparallel alignment.

The theoretical description is based on toy models relying on a series of simplifying assumptions. The initial electrical circuit is replaced by nodes interconnected by tunnel matrix elements [10]. Each node corresponds to a large quantum dot so that the energy levels form a continuum within each node. We suppose that the propagators within a given node are uniform in space. A ferromagnetic node is thus characterized as the spin-up and spin-down density of state. A superconducting node is characterized by the ordinary and anomalous propagators. We suppose that the applied voltages are small compared to the superconducting gap and that the propagators at a given node are independent of energy. Each node is supposed to be in local equilibrium so that the distribution function within each node is represented by the Fermi–Dirac distribution. To impose Kirchoff laws, we determine the spin-up and spin-down chemical potentials so that the spin-up and spin-down currents are conserved at each node [10].

2. M/M/M junction

Let us first consider the metal/metal/metal junction in figure 1, in which we suppose that a large quantum dot (node x) is inserted between two metallic electrodes represented by nodes α and β. We first calculate the Green functions $G_{i,j}$ of the connected system that are the solution of the chain of Dyson equations given by $G = g + g \otimes \Sigma \otimes G$ in a compact notation [11], where Σ is the self-energy that contains all couplings of

$$\mathcal{W} = t_{\alpha,x} c_\alpha^+ c_x + t_{x,\alpha} c_x^+ c_\alpha + t_{\beta,x} c_\beta^+ c_x + t_{x,\beta} c_x^+ c_\beta. \tag{1}$$

The coupling Hamiltonian (1) is formally equivalent to a tunnelling Hamiltonian but similarly to [12], we use a non-perturbative method based on [11] that is valid also for large interface transparencies. This method avoids inconsistencies present in the tunnelling Hamiltonian model in the regime of high transparency interfaces [13]. The symbol $\otimes$ in the Dyson equation includes a convolution over time arguments and a summation over the labels of the network. Since there is no magnetic flux one has $t_{\alpha,x} = t_{x,\alpha}$ and $t_{x,\beta} = t_{\beta,x}$. To obtain the current flowing from node α to node x we evaluate the Keldysh Green functions given by $G^{+,-} = (1 + G^{\mathrm{R}} \otimes \Sigma) \otimes g^{+,-} \otimes (1 + \Sigma \otimes G^{\mathrm{A}})$ [11, 12], where the symbols A and R stand for advanced and retarded. The current is related to the Keldysh Green function by the relation [11]

$$I_{\alpha,x} = \frac{e^2}{h} \int [t_{\alpha,x} G^{+,-}_{x,\alpha}(\omega) - t_{x,\alpha} G^{+,-}_{\alpha,x}(\omega)] \, \mathrm{d}\omega. \tag{2}$$

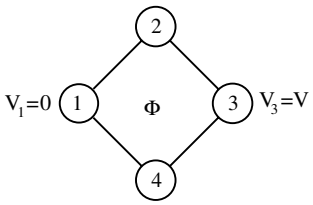

Figure 2. The toy model used to discuss Aharonov–Bohm oscillations. A voltage $V_1 = 0$ is applied on node 1 and a voltage $V_3 = V$ is applied on node 3. The chemical potentials at nodes 2 and 4 are determined in such a way that current is conserved.

The current flowing from node α to node x is given by

$$I_{\alpha,x} = \frac{4\pi^2 t_{\alpha,x}^2 \rho_\alpha \rho_x}{\mathcal{D}^2}(\mu_x - \mu_\alpha) + \frac{4\pi^4 t_{\alpha,x}^2 t_{\beta,x}^2 \rho_\alpha \rho_\beta \rho_x^2}{\mathcal{D}^2}(\mu_\beta - \mu_\alpha), \tag{3}$$

with $\mathcal{D} = 1 + \pi^2 t_{x,\alpha}^2 \rho_\alpha \rho_x + \pi^2 t_{x,\beta}^2 \rho_\beta \rho_x$. The current flowing from node x to node β is obtained by exchanging the labels α and β and changing sign. The chemical potential μ_x in the intermediate region is deduced from the Kirchoff law $I_{\alpha,x} = I_{x,\beta}$:

$$\mu_x = \frac{t_{\alpha,x}^2 \rho_\alpha \mu_\alpha + t_{\beta,x}^2 \rho_\beta \mu_\beta}{t_{\alpha,x}^2 \rho_\alpha + t_{\beta,x}^2 \rho_\beta}. \tag{4}$$

As expected if $t_{\alpha,x} = t_{\beta,x}$ and if $\rho_\alpha = \rho_\beta$ we obtain $\mu_x = \frac{1}{2}(\mu_\alpha + \mu_\beta)$. The conductance $G = \mathrm{d}I/\mathrm{d}V(V = 0)$ is obtained by replacing the value of the chemical potential (4) in the expression of the current equation (3):

$$G = \frac{e^2}{h} \frac{4\pi^4 t_{\alpha,x}^2 t_{\beta,x}^2 \rho_\alpha \rho_\beta \rho_x^2}{\mathcal{D}^2} \left[1 + \frac{1}{\pi^2 t_{\alpha,x}^2 \rho_\alpha \rho_x + \pi^2 t_{\beta,x}^2 \rho_\beta \rho_x} \right]. \tag{5}$$

We recognize a contribution due to elastic cotunnelling and a contribution due to sequential tunnelling.

3. Aharonov–Bohm oscillations in normal structures

To discuss Aharonov–Bohm oscillations we consider the toy model in figure 2. We consider a symmetric structure in which $\rho = \rho_1 = \rho_3$ and $\rho' = \rho_2 = \rho_4$, and we use the notation $u = \pi^2 t^2 \rho \rho'$. The conductance is given by

$$G = \frac{e^2}{h} \frac{4u}{1 + 4u + 2u^2(1 - \cos \Phi)} \tag{6}$$

which oscillates with the applied magnetic flux. As a consequence our toy model can be used to describe Aharonov–Bohm oscillations.

4. Crossed Andreev reflection

Now we discuss crossed Andreev reflection [1–3]. We consider the same toy model as in figure 1 but now node x is superconducting. We denote by $\rho_\alpha^\uparrow$, $\rho_\alpha^\downarrow$, $\rho_\beta^\uparrow$ and $\rho_\beta^\downarrow$ the density of states of spin-up and spin-down electrons in electrodes α and β. We call g the ordinary propagator of the superconducting node and f the anomalous propagator. We show that f

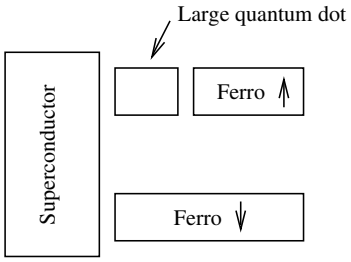

Figure 3. Geometry of the device in which a large quantum dot is inserted into a crossed Andreev reflection circuit.

and g should satisfy the relation $f^2 = g^2$. Solving the Dyson equation and evaluating the Dyson–Keldysh equation leads to the transport formula

$$I^{\uparrow}_{\alpha,x} = -\frac{2e^2}{h} V_\alpha \frac{4\pi^2 t^4_{x,\alpha}}{\mathcal{D}^{\mathrm{A}}\mathcal{D}^{\mathrm{R}}} f^2 \rho^{\uparrow}_\alpha \rho^{\downarrow}_\alpha \tag{7}$$

$$- \frac{e^2}{h}(V_\alpha - V_\beta) \frac{4\pi^2 t^2_{x,\alpha} t^2_{x,\beta}}{\mathcal{D}^{\mathrm{A}}\mathcal{D}^{\mathrm{R}}} |g^{\downarrow}|^2 \rho^{\uparrow}_\alpha \rho^{\uparrow}_\beta \tag{8}$$

$$- \frac{e^2}{h}(V_\alpha + V_\beta) \frac{4\pi^2 t^2_{x,\alpha} t^2_{x,\beta}}{\mathcal{D}^{\mathrm{A}}\mathcal{D}^{\mathrm{R}}} f^2 \rho^{\uparrow}_\alpha \rho^{\downarrow}_\beta, \tag{9}$$

where the determinant $\mathcal{D}$ is given by $\mathcal{D}^{\mathrm{A}} = 1 - \mathrm{i}\pi g(\Gamma^{\uparrow} + \Gamma^{\downarrow}) + \pi^2(f^2 - g^2)\Gamma^{\uparrow}\Gamma^{\downarrow}$, and where $\Gamma^{\uparrow} = |t_{x,\alpha}|^2\rho^{\uparrow}_\alpha + |t_{x,\beta}|^2\rho^{\uparrow}_\beta$ and $\Gamma^{\downarrow} = |t_{x,\alpha}|^2\rho^{\downarrow}_\alpha + |t_{x,\beta}|^2\rho^{\downarrow}_\beta$. The function $g^{\downarrow}$ is given by $g^{\downarrow} = g + \mathrm{i}\pi(f^2 - g^2)\Gamma^{\downarrow}$. The term (7) corresponds to local Andreev reflections, the term (8) corresponds to elastic cotunnelling and the term (9) corresponds to crossed Andreev reflection. In microscopic models it is possible to show that, because of averaging between the different conduction channels, the conductance associated with crossed Andreev reflection is equal to the conductance associated with elastic cotunnelling [2, 3]. This cannot be demonstrated in our toy model because we lost all information about the spatial dependence of the propagators in the superconductor. Instead we choose the propagators f and g in such a way that the conductance associated with elastic cotunnelling is identical to the conductance associated with crossed Andreev reflection. This leads to the condition $f^2 = g^2$. This condition ensures the equality of the Andreev reflection and elastic cotunnelling currents also for large interface transparencies.

5. Effect of an out-of-equilibrium conductor

Now we discuss a device containing a large quantum dot inserted into a crossed Andreev reflection circuit. The non-equilibrium effects are described by the out-of-equilibrium distribution function $n_{\mathrm{F}}(\omega - \mu_{i,\sigma})$ where $\mu_{i,\sigma}$ is equal to the local chemical potential of spin-σ electrons in node i. The values of $\mu_{i,\sigma}$ are determined in such a way that current is conserved. The geometry of the device is shown in figure 3 and the toy model is shown on figure 4. Without the quantum dot the current response is symmetric: for the toy model in figure 1 with node x being superconducting, the crossed conductance $\mathcal{G}_{\alpha,\beta} = \partial I_\alpha(V_\alpha, V_\beta)/\partial V_\beta$ is equal to $\mathcal{G}_{\beta,\alpha} = \partial I_\beta(V_\beta, V_\alpha)/\partial V_\alpha$ [2, 3]. As figure 5 shows, such symmetry relations are not valid for the device in figure 3. With the parameters in figure 5, we see that the total density of states at nodes 2 and 3 is equal to $1 + y$. The absolute value of the density of states ρ can be larger than unity.

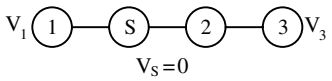

Figure 4. The toy model corresponding to figure 3. Node 1 corresponds to the spin-down electrode in figure 3. Node 3 corresponds to the spin-up electrode and node 2 corresponds to the large quantum dot.

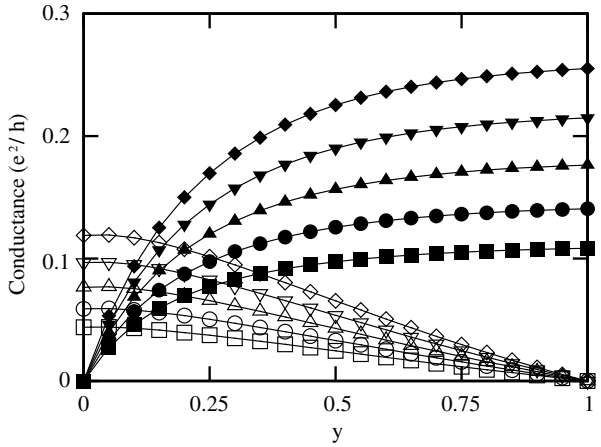

Figure 5. Comparison between the crossed conductances in two situations for the toy model in figure 4: (i) $V_1 = 0$ and $V_3 = V$ (open symbols); and (ii) $V_1 = V$ and $V_3 = 0$ (filled symbols). The densities of states are given by $\rho_N = 1$, $\rho_{1,\uparrow} = 1$, $\rho_{1,\downarrow} = 0$, $\rho_{2,\uparrow} = y$, $\rho_{2,\downarrow} = 1$, $\rho_{3,\uparrow} = y$ and $\rho_{3,\downarrow} = 1$. The different curves correspond to different values of the hopping parameter: $t = 0.11$ (□ and ■); $t = 0.12$ (○ and ●); $t = 0.13$ (△ and ▲); $t = 0.14$ (▽ and ▼); $t = 0.15$ (◇ and ◆).

Generically if the densities of states increase at one point we will be out of the convergence radius of the perturbative series (namely the term of order t^4 becomes larger than the term of order t^2, the term of order t^6 becomes larger than the term of order t^4, etc), but the values of the tunnel matrix elements are small enough so that we are not in this regime.

The limiting cases $y = 0$ and 1 can be understood on simple grounds (see figure 5). For $y = 0$, node 1 is a half-metal spin-up ferromagnet (meaning that only spin-up electrons are present in node 1) and nodes 2 and 3 are half-metal spin-down ferromagnets. If we suppose that $V_1 = V \neq 0$ and $V_3 = V_S = 0$ we see that there is no voltage difference between the superconductor and node 3. As a consequence the spin-down electrons arising from crossed Andreev reflection cannot be transmitted to node 3 and give rise to charge accumulation at node 2. There is no current in this case. If we suppose that $V_1 = 0$, $V_3 = V \neq 0$ and $V_S = 0$ we see that spin-down electrons arising from crossed Andreev reflection can be transmitted to node 3 because there is a voltage difference between the superconductor and node 3. There is a finite current, in agreement with figure 5.

Another limiting case is $y = 1$ (see figure 5). For $y = 1$ node 1 is a half-metal spin-up ferromagnet, nodes 2 and 3 are normal metal. We find that the crossed conductance is finite if $V_1 = V \neq 0$, $V_3 = 0$ and is zero if $V_1 = 0$ and $V_3 = V \neq 0$ (see figure 5). This should be contrasted with the case $y = 0$ where the opposite occurs. The case $V_1 = 0$, $V_3 = V \neq 0$ can be understood from a cancellation between the currents due to crossed Andreev reflection and elastic cotunnelling so that the crossed conductance is zero, unlike the case $y = 0$ discussed above. The case $V_1 = V \neq 0$, $V_3 = 0$ is more complex because it involves spin accumulation

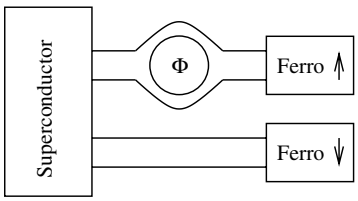

Figure 6. Geometry of the Aharonov–Bohm experiment.

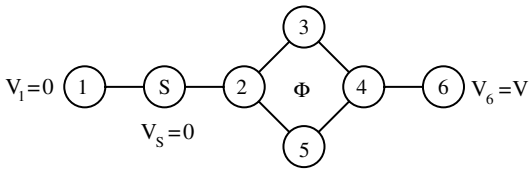

Figure 7. The toy model used to discuss the Aharonov–Bohm experiment represented on figure 6.

at node 2 in the presence of elastic cotunnelling and crossed Andreev reflection. Spin-up electrons from node 2 are transferred to node 1 by elastic cotunnelling. Due to crossed Andreev reflection, spin-up electrons are transferred to node 1 and spin-down electrons are transferred to node 2. The rate of the two processes is identical and there is thus no charge accumulation like in the case $y = 0$ discussed above. A naive argument would suggest that the spin-up and spin-down chemical potentials at node 2 take opposite values and that no charge current is flowing from node 2 to node 3, but only a spin current is flowing. As seen in figure 5, this is not the case since we find a finite charge current flowing from node 2 to node 3. We suggest that the naive reasoning does not work because the distribution function at node 2 may be affected by the fact that the two electrons arising from crossed Andreev reflection have an opposite energy, whereas elastic cotunnelling is at constant a energy. This may induce a non-trivial distribution function at node 2.

6. Aharonov–Bohm effect related to pair states

Now we consider the device in figure 6 in which an Aharonov–Bohm loop is inserted in a crossed Andreev reflection circuit and we use the toy model in figure 7. We first consider that the Aharonov–Bohm loop is a half-metal ferromagnet. In this case the only phenomenon at work is crossed Andreev reflection for antiparallel spin orientations and elastic cotunnelling for parallel spin orientations. We obtain Aharonov–Bohm oscillations with a negative magnetoresistance (see figure 8). It may be difficult to probe these situations in experiments because the phase coherence length in ferromagnetic metals is very small. This is why we consider the case where the Aharonov–Bohm loop is made of a normal metal.

Several phenomena come into play:

(i) crossed Andreev reflection;
(ii) elastic cotunnelling;
(iii) spin accumulation in the Aharonov–Bohm loop (the local spin-up and spin-down chemical potentials are not equal);
(iv) electroflux effect similar to [14] (the local chemical potential oscillates with the magnetic flux applied on the Aharonov–Bohm loop).

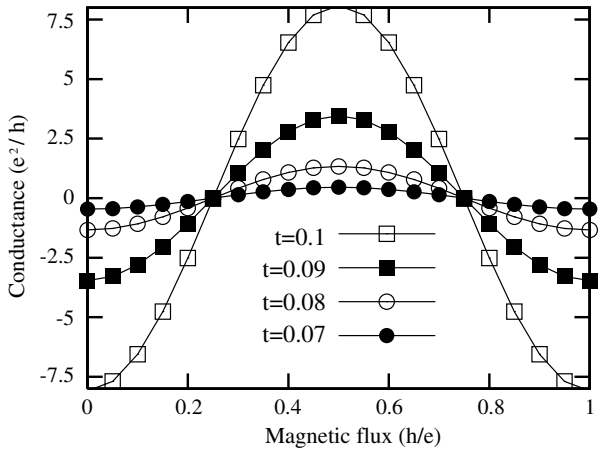

Figure 8. Aharonov–Bohm effect related to non-separable correlations. Node 1 is a half-metal spin-up ferromagnet and the Aharonov–Bohm loop is a half-metal spin-down ferromagnet: $\rho_{i,\uparrow} = 1$ and $\rho_{i,\downarrow} = 0, i = 2, \ldots, 6$. We have shown the variation of $G_{S,1}(\Phi) - G^{av}_{S,1}$ as a function of Φ. The average conductance defined as $G^{av}_{S,1} = (G_{S,1}(\Phi = 0) + G_{S,1}(\Phi = \pi))/2$ is positive. The tunnel amplitudes are identical for all links of the network: $t = 0.1$ (□); $t = 0.09$ (■); $t = 0.08$ (○); $t = 0.07$ (●). We obtain the same oscillations with a parallel spin orientation of the ferromagnetic electrodes but with an opposite current.

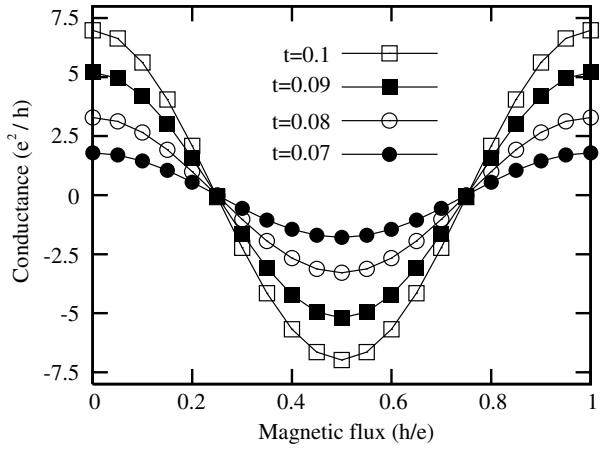

Figure 9. The same as figure 8, but now nodes $2, \ldots, 5$ are unpolarized: $\rho_{i,\uparrow} = \rho_{i,\downarrow} = 1$ with $i = 2, \ldots, 5$.

Another possible process occurring in this structure with highly transparent interfaces is that the two electrons of a Cooper pair are transferred into the Aharonov–Bohm loop, couple to the magnetic flux and come back in the other electrode. As figure 9 shows, we also obtain Aharonov–Bohm oscillations but with a positive magnetoresistance.

7. Conclusion

To summarize, we have provided a toy model of multiterminal hybrid structures containing large quantum dots. We applied the model to a device in which a large quantum dot is inserted

into a crossed Andreev reflection circuit. We also proposed another possible experiment intended to probe an Aharonov–Bohm effect related to spatially separated pairs of electrons. These two situations may be the object of future experiments. The description was based on a toy model in which the initial electrical circuit is replaced by a set of nodes interconnected by tunnel matrix elements. It is expected that the qualitative behaviour is captured by our toy model. The formulation of a microscopic theory is left as an important open question. Within a microscopic theory it would be possible to discuss rigorously the role played by the elastic mean free path and the phase coherence length. In our toy model each node is described by a single propagator. As a consequence we have lost all information about the spatial variation of the propagators and we suppose implicitly that the distance between the contacts is smaller than the elastic mean free path. But qualitatively for the device in figure 6, the current is proportional to the square of the anomalous propagator in the superconductor, and to the square of the ordinary propagator in the normal metal electrodes. We have supposed in our toy model that the distance D between the contacts on the superconductor is much smaller than the BCS coherence length ξ_{BCS} and the length R of the normal metal electrodes is much smaller than the phase coherence length l_ϕ. Qualitatively the conductances in figures 5, 8 and 9 should thus be multiplied by the exponential factors $\exp(-D/\xi_{\mathrm{BCS}})$ and $\exp(-R/l_\phi)$. Another important ingredient is the role played by interface transparencies. We could solve the toy model with arbitrary interface transparencies and obtain in some cases a crossed conductance larger than e^2/h with large interface transparencies. As discussed previously, the value of the conductance would be much smaller in a microscopic model because of the exponential dependence of the propagators in the superconductor. More realistically, it would also be interesting to discuss diffusive models in connection with the occurrence of h/e oscillations in the conductance predicted from the toy model. h/e oscillations have been also obtained for the proximity effect in other geometries (see [15]).

Acknowledgment

The authors acknowledge fruitful discussions with D Feinberg.

References

[1] Deutscher G and Feinberg D 2000 *Appl. Phys. Lett.* **76** 487
[2] Falci G, Feinberg D and Hekking F W J 2001 *Europhys. Lett.* **54** 255
[3] Mélin R and Feinberg D 2002 *Eur. Phys. J.* B **26** 101
[4] Lesovik G B, Martin T and Blatter G 2001 *Eur. Phys. J.* B **24** 287
[5] Choi M S, Bruder C and Loss D 2000 *Phys. Rev.* B **62** 13569
Recher P, Sukhorukov E V and Loss D 2001 *Phys. Rev.* B **63** 165314
Recher P and Loss D 2002 *Preprint* cond-mat/0205484
Saraga D S and Loss D 2002 *Preprint* cond-mat/0205553
[6] Mélin R 2001 *J. Phys.: Condens. Matter* **13** 6445
[7] Sauret O, Feinberg D and Martin T 2002 *Preprint* cond-mat/0203215
[8] Bouchiat V, Chtchelkatchev N, Feinberg D, Lesovik G B, Martin T and Torrès J 2002 *Preprint* cond-mat/0206005
[9] Giroud M, Hasselbach K, Courtois H, Mailly D and Pannetier B 2002 *Preprint* cond-mat/0204140
[10] Nazarov Y V 1994 *Phys. Rev. Lett.* **73** 1420
Nazarov Y V 1999 *Superlatt. Microstruct.* **25** 1221
[11] Caroli C, Combescot R, Nozières P and Saint-James D 1971 *J. Phys. C: Solid State Phys.* **4** 916
Caroli C, Combescot R, Nozières P and Saint-James D 1972 *J. Phys. C: Solid State Phys.* **5** 21
[12] Cuevas J C, Martin-Rodero A and Yeyati A L 1996 *Phys. Rev.* B **54** 736
[13] Burstein E and Lundqvist S 1969 *Tunneling Phenomena in Solids* (New York: Plenum)
[14] Stoof T H and Nazarov Y V 1996 *Phys. Rev.* B **54** R772
[15] Yoshioka H and Fukuyama H 1991 *Physica* C **185–189** 1625